Supporting Information

Strong Absorption Enhancement in Si Nanorods

Ilya Sychugov,*,† Fatemeh Sangghaleh,† Benjamin Bruhn,† Federico Pevere,†
Jun-Wei Luo,*,‡ Alex Zunger,§ and Jan Linnros†

†*Materials and Nano Physics Department, KTH – Royal Institute of Technology, Kista, Stockholm, 16440, Sweden*

‡*State Key Laboratory for Superlattices and Microstructures, Institute of Semiconductors, Chinese Academy of Sciences, P.O. Box 912, Beijing 100083, China*

§*Renewable and Sustainable Energy Institute, University of Colorado, Boulder, Colorado 80309, USA*

Sample fabrication. Individual silicon nanorods in an oxide matrix were made by lithography, plasma etching and oxidation (900°C, 6 hrs.) of silicon nanowalls. The nanowalls were ~ 100 nm wide and ~ 200 nm tall, prepared from low-doped silicon wafers.[21] The elongated geometry of nanoparticles (Figure S1, left) originated from discontinuities in the oxidation of a silicon nanowire in the top of the nanowalls.[25] The nanorods are elongated along <110> crystallographic axis, as defined by the direction of lithographical patterning of original nanowalls. Close-to-spherical particles for single-dot studies were prepared by oxidation (900°C, 1 min.) of thin SOI layers. High resolution transmission electron microscope (HRTEM) images revealed nanocrystals with a shape close to spherical, as well as faceted nanoparticles (Figure S1, right).[26-27] Fourier analysis reveals no significant strain in both single nanorod and nanodot samples: the interplanar distance for (111) planes measured to be 3.20±0.03 nm^{-1}, similar to the bulk value of 3.19 nm^{-1} (Figure S1, bottom).

* Corresponding authors: ilyas@kth.se, jwluo@semi.ac.cn

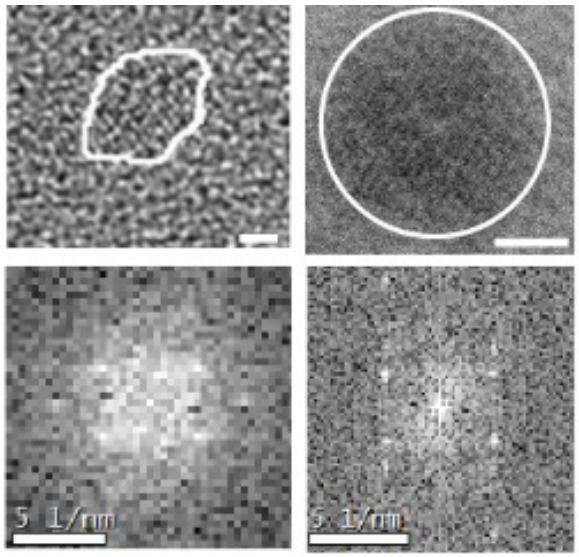

Figure S1. *(top) HRTEM images of a nanorod (adapted from [S4]. Copyright 2013 by the American Physical Society) and a nanodot (reprinted with permission from [S5]. Copyright 2010 IOP Publishing). Scale bar is 2 nm. (bottom) Fourier transforms of the TEM images of (left) the nanorod and (right) the nanodot. The interplanar distance of (111) planes in silicon in the reciprocal space is 3.19 nm^{-1}; in both images the measured interplanar distance is 3.20±0.03 nm^{-1}, indicating low strain in the nanocrystals.*

For the ensemble sample of close-to-spherical particles the implantation of Si^+ to ~ 100 nm thick SiO_2 with subsequent annealing was used.[S1] The particles produced by this method are known to be close-to-spherical in shape, as evidenced by numerous TEM observations.[S2-S3]

The oxide layer with embedded nanocrystals was then patterned and etched ~ 100 nm to the substrate to replicate the nanowall geometry of the lithography-defined nanorod sample (Figure S2). This was done to independently verify whether one-dimensional nanowalls themselves induce any effect on absorption in nanoparticles.

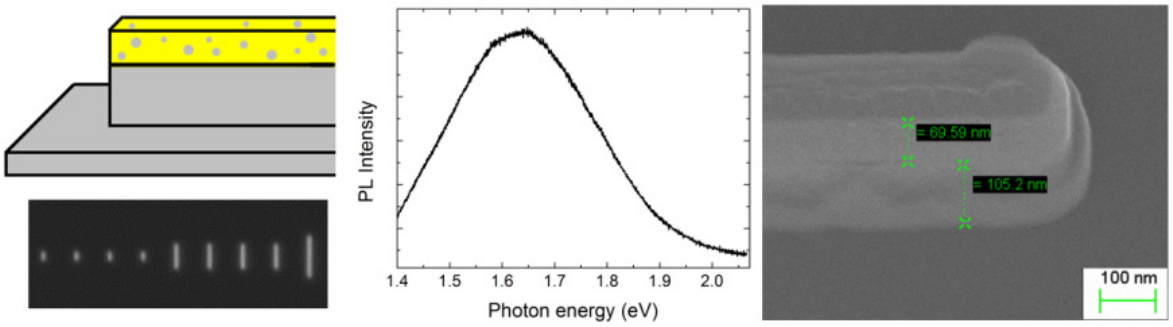

Figure S2. *(left) Schematics of the reference sample of ensemble of spherical NCs in nanowalls prepared by implantation and annealing with corresponding PL image (~ 15x50 μm^2 area) below. Different length nanowalls were prepared; (middle) Photoluminescence spectrum of these nanocrystals. (Right) SEM image of nanowalls with spherical nanocrystals: the top layer is nanocrystal-rich SiO_2 and the bottom layer is Si.*

Polarization-dependent measurements on single nanoparticles. The samples were placed on an inverted wide-field microscope (Zeiss) and excited using epifluorescence (bright-field) geometry by a 405 nm laser diode (Omicron), which generates a vertically polarized beam (polarization ratio > 100:1). The emitted light was collected by a X100 objective lens (long working distance, 0.73 NA) and detected by a thermoelectrically cooled CCD camera (Andor, iXon3). An example of the polarization-dependent absorption curve for a nanorod is shown in Fig. S3.

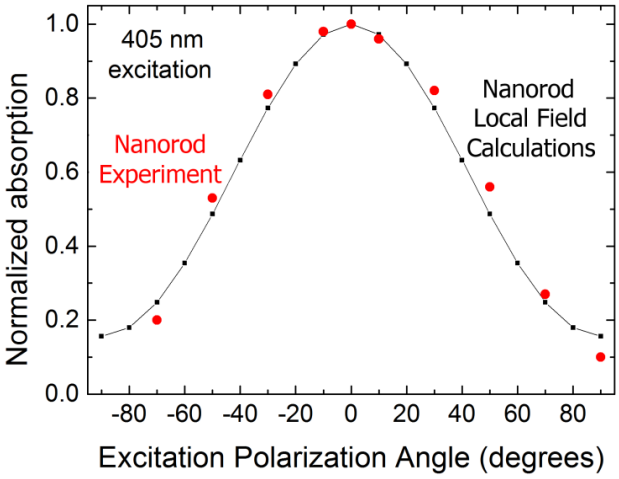

Figure S3. *Measured absorption dependence on the excitation polarization for a single Si nanorod (red circles) and local field calculations for a ~ 1.1×1.1×2.8 nm semi axes Si ellipsoid (black) under 405 nm excitation. Polarization angle is the angle between the electric field vector and the ellipsoid long axis (nanowall direction).*

Absorption curve measurements on single nanoparticles. To obtain the excitation energy dependence of absorption, we performed photoluminescence excitation measurements. A Laser-driven Xe lamp (Energetic) with an attached wavelength-selecting monochromator (Princeton Instruments) was used for the excitation below the photoluminescence saturation regime. The spectral resolution of the excitation beam was ~ 6 nm (20 – 60 meV in the probed spectral range 2.0 – 3.5 eV), which allowed to collect at least 35-40 data points for the absorption curve. The beam was focused to a spot of ~ 30 μm diameter, where a quantum dot of interest was moved to using a remote micro-positioning system. Examples of such PL images for both nanorod and nanodot samples are given in Figure 1.

The PL signal was then extracted from the recorded images for every excitation wavelength by integrating the signal area (~ 6×6 pixels) and subtracting the background extracted from the region next to the quantum dot. The absorption cross-section energy dependence was obtained from the recorded PL signal by correcting it to the excitation power density at each wavelength.

Absorption cross-section measurements on single nanoparticles. To calibrate the obtained absorption curves we measured luminescence decay and rise times under modulated 405 nm laser diode excitation of varying power. Since the non-polarized light from the wavelength-selected xenon lamp is difficult to modulate with necessary parameters (<100 ns rise time and >10 kHz repetition rate) here we relied on the polarized laser excitation. In this experiment the PL signal was collected by an avalanche photodiode (ID Quantique) connected to another output port of the same microscope.[31] Then, from population rate equations, the luminescence rise rate Γ_{rise} can be shown to be directly proportional to the excitation photon flux Φ_{exc}:

$$\Gamma_{rise} = \sigma \cdot \Phi_{exc} + \Gamma_{decay} \quad \text{(S1)},$$

where Γ_{decay} is the luminescence decay rate.[34] Thus, the slope of this linear dependence yields the absorption cross-section σ.[31] To reduce background luminescence in this experiment, dark field excitation geometry was used. The incident beam impinged at 20^o from the sample surface and at 45^o to the nanowall direction, corresponding to ~ 70^o bright field polarization angle (see reasoning behind the choice of this angle in the main text).

Classical calculation of the local field effect. Simulations for Si nanocrystals embedded in silica were performed by numerically solving Maxwell equations in 3D for the propagating electromagnetic monochromatic wave of a wavelength λ_0:

$$\nabla \times \nabla \times \mathbf{E} - k_0^2 \varepsilon_r \mathbf{E} = 0 \quad \text{(S2)},$$

where **E** is electric field, k_0 is a wave vector: $k_0 = 2\pi/\lambda_0$, and ε_r is the energy-dependent relative permittivity: $\varepsilon_r = (n - ik)^2$. Energy-dependent bulk values of *n* and *k* for silicon were used.[S6] The incoming energy flux density was set to be the same for all configurations and the total dissipated power in the particle served as a measure of absorption (Figs. S4, S5).

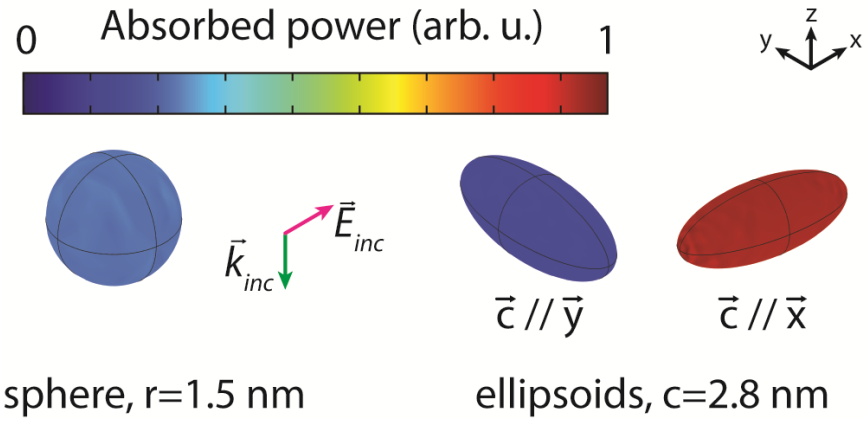

Figure S4. *Calculated absorbed power for a Si sphere and ellipsoids of the same volume oriented parallel and perpendicular to the electric field (along y- and x-axes). The incident electric field is polarized along x- and travels along z-direction (405 nm wavelength in air). The absorption is slightly reduced in the nanorods perpendicular to the field and is strongly enhanced for the aligned ellipsoids relative to the spherical particle.*

Calculations were made for different nanoparticle geometries and polarizations, using a classic continuum approach in COMSOL software.

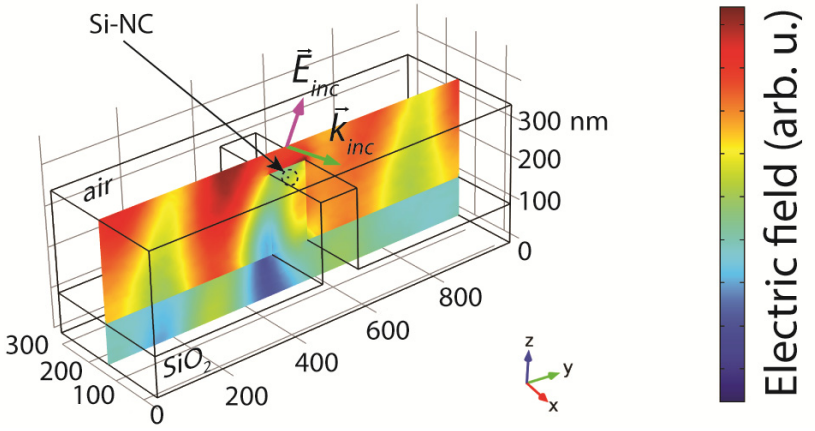

Figure S5. *Simulated field distribution for the experimental geometry for Si nanorods embedded in oxide nanowalls under dark field excitation (the field is impinging at 45° azimuthal angle and at 20° elevation angle). This configuration is equivalent to ~ 70° angle between the electric field and the nanorod long axis for the bright field excitation regime in terms of absorbed power.*

Atomistic calculation of the quantum mechanical electronic structure. The single particle eigenstates (ε_i; $\psi_i(\boldsymbol{r})$) of differently shaped Si NCs were obtained from direct diagonalization, in a basis set of plane-wave functions, of the Schrödinger equation.[6] The crystal potential of the NC plus its matrix are both described as a superposition of atomic screened (semi-empirical pseudopotential) potentials υ_α of atom type at each atomic site $\mathbf{R}_{\alpha,n}$ within the lattice site *n*: $V(\mathbf{r}) = \sum_{\alpha,n} \upsilon_\alpha\left(\mathbf{r} - \mathbf{R}_{\alpha,n}\right)$. The semi-empirical pseudopotential method takes into account inter-band coupling, inter-valley coupling (coupling between different parts of the Brillouin zone), and spin orbit coupling.[29] For the modeling of the matrix a fictitious, lattice-matched barrier material having a wide bandgap was introduced. The matrix material reproducing the experimentally measured bandgap of Si QDs in SiO_2 in a wide energy range was used.[6]

This method was shown to be more accurate than continuum-based approaches, such as effective mass approximation, both for nanocrystals and nanowires.[30, S7] The no-phonon optical absorption spectrum $\alpha(\hbar\omega)$ in single-particle basis is then calculated, given the dipole transition matrix $\overline{P}_{vc} =< v|\hat{e}\cdot\mathbf{p}|c >$, according to Fermi's golden rule:

$$\alpha(\hbar\omega) = \left(\frac{2\pi e}{m_0\omega}\right)^2 \sum_v \sum_c |\overline{P}_{vc}|^2 exp\left[-\left(\frac{\hbar\omega - E_{vc}}{\lambda}\right)^2\right] \qquad \text{(S3).}$$

Here $E_{vc} = E_c - E_v$ is the transition energy from hole state *v* to electron state *c*, m_0 is the free-electron mass, *e* is the free-electron charge, and λ represents the spectral line broadening. The value of the broadening in calculations of the absorption curve was set to 50 meV. It corresponds to the experimental conditions of the convoluted broadening from the 20-60 meV probe energy resolution and ~ 25 meV thermal broadening (all measurements were performed at room temperature). Examples of the obtained absorption curves for a spherical particle and nanorods of the same volume are shown in Figure S6.

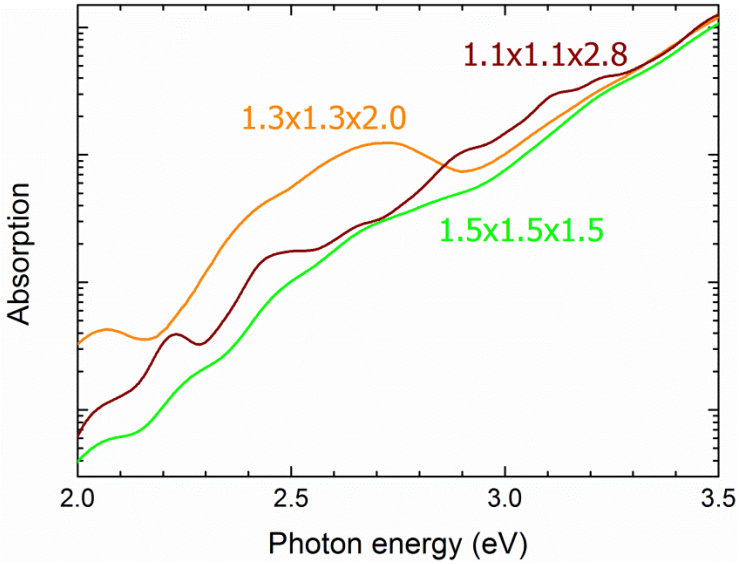

Figure S6. *Calculated absorption curves by the atomistic pseudopotential method for a spherical silicon nanocrystal of 3 nm diameter (adapted from [S8], copyright by the American Physical Society) and for nanorods with 1.3×1.3×2 nm and 1.1×1.1×2.8 nm semi axes. Broadening was set to be 50 meV, corresponding to the experimental conditions.*

References

S1. Chulapakorn, T.; Sychugov, I.; Suvanam, S.; Linnros, J.; Wolff, M.; Primetzhofer, D.; Possnert, G.; Hallén, A., *Phys. Status Solidi C* **2015,** *12*, 1301-1305.

S2. Guha, S.; Pace, M. D.; Dunn, D. N.; Singer, I. L., *Appl. Phys. Lett.* **1997,** *70*, 1207-1209.

S3. Fujii, M.; Kanzawa, Y.; Hayashi, S.; Yamamoto, K., *Phys. Rev. B* **1996,** *54*, R8373-R8376.

S4. Bruhn, B.; Valenta, J.; Sychugov, I.; Mitsuishi, K.; Linnros, J., *Phys. Rev. B* **2013,** *87*, 045404.

S5. Sychugov, I.; Nakayama, Y.; Mitsuishi, K., *Nanotechnology* **2010,** *21*, 5 285307.

S6. Green, M. A., *Sol. Energy Mater. Sol. Cells* **2008,** *92*, 1305-1310.

S7. Luo, J. W.; Li, S. S.; Xia, J. B.; Wang, L. W., *Appl. Phys. Lett.* **2006,** *88*, 143108

S8. Sychugov, I.; Pevere, F.; Luo, J. W.; Zunger, A.; Linnros, J., *Phys. Rev. B* **2016,** *93*, 161413(R).